JOURNAL OF Materials CHEMISTRY

Structural studies on amorphous silicon boron nitride $Si_3B_3N_7$: neutron contrast technique on nitrogen and high energy X-ray diffraction

Ralf M. Hagenmayer,[a] Utz Müller,[b] Chris J. Benmore,[c] Jörg Neuefeind[d] and Martin Jansen*[a]

[a]*Max-Planck-Institut für Festkörperforschung, Heisenbergstr. 1, 70569 Stuttgart, Germany. E-mail: martin@jansen.mpi-stuttgart.mpg.de*
[b]*Institut für Anorganische Chemie, Universität Bonn, Gerhard-Domagk-Str. 1, 53121 Bonn, Germany*
[c]*ISIS Facility, Rutherford Appleton Laboratory, Chilton, Didcot, Oxon, UK OX11 0QX*
[d]*HASYLAB at DESY, Notkestr. 85, 22603 Hamburg, Germany*

Received 24th March 1999, Accepted 16th August 1999

The structure of the new ternary amorphous nitride $Si_3B_3N_7$, synthesised from the single source precursor TADB [(trichlorosilyl)aminodichloroborane], has been investigated by means of X-ray diffraction using high energy synchrotron radiation and by neutron diffraction using the isotopic contrast technique on nitrogen. The X-ray results have been compared with results from electron diffraction experiments, confirming the trigonal planar coordination of boron ($R_{BN}=1.4$ Å, $Z_{BN}=2.8$, $Z_{NB}=1.2$) by nitrogen and the tetrahedral coordination of silicon ($R_{SiN}=1.7$ Å, $Z_{SiN}=3.8$, $Z_{NSi}=1.6$) by nitrogen. The neutron contrast technique was applied in order to obtain detailed information about the nitrogen environment. From the total pair correlation functions the N–N distances within the boron and silicon coordination polyhedra could be extracted [$R_{NN}(B)=2.5$ Å, $R_{NN}(Si)=2.8$ Å]. In addition, the difference function shows two distinct maxima at *ca.* 3.8 and 4.3 Å in the third coordination sphere resulting from Si–N or B–N pairs connected *via* three bonds. If at least two of these are B–N bonds a contribution to the first peak results, while the second maximum is matched if at least two Si–N bonds are involved.

Introduction

Recently synthesised multinary amorphous nitridic ceramics show improved properties in comparison with their binary crystalline components.[1] While syntheses of multinary oxides usually can be achieved by co-milling and heating of the respective binary reactants, this all-solid-state route is not applicable to ceramic nitrides, mainly because of the low diffusion coefficients of silicon or boron in their respective binary nitrides. However, starting the synthesis with a single source precursor has proven to be a viable and versatile approach.[2]

To fabricate amorphous silicon boron nitrides or carbonitrides we chose the precursor $Cl_3Si–NH–BCl_2$ [TADB = (trichlorosilyl)aminodichloroborane]. Depending on the conditions maintained during polymerisation and pyrolysis we can produce either the carbonitride $SiBN_3C$ or the carbon free ternary phase $Si_3B_3N_7$[3] (Scheme 1).

MAS NMR measurements have been performed[3,4] in order to determine the local environments of the constituent elements. The ^{29}Si spectra of both ceramics indicate that the silicon atoms are tetrahedrally coordinated by four nitrogen atoms. The ^{11}B spectra are typical for a trigonal planar environment for boron, whereas the ^{15}N measurements give a broad signal which mainly reflects the amorphous character of the samples. Although the range in the observed chemical shift is broad, the presence of tetrahedrally coordinated nitrogen can be excluded for both ceramics.

Diffraction experiments on amorphous materials give information on short-range and medium-range order. Fourier transformation of the corrected and normalised intensity leads to total correlation functions describing the distribution of all atomic pairs, however, these total correlation functions are a weighted sum of partial functions, each representing an atomic pair distribution. Neutron diffraction using isotopic substitution is a very powerful method to extract these partial functions in binary amorphous alloys.[5] Recently this approach has been extended to systems with more than two components.[6] With properly chosen isotopes showing significant differences in the scattering lengths, differential pair correlation functions are accessible. For $Si_3B_3N_7$, the isotopic pair ^{15}N and ^{14}N meets this condition pretty well [$b(^{14}N)=9.37(2)$ fm, $b(^{15}N)=6.44(3)$ fm[7]]. Since we are studying a ternary system, only six rather than ten partial functions (for a quaternary system) needed to be considered. $Si_3{}^{11}B_3{}^{nat}N_7$ and $Si_3{}^{11}B_3{}^{15}N_7$ synthesised starting from ^{nat}N-ammonia or ^{15}N-ammonia and ^{11}B-boric acid. Details and further IR and NMR spectroscopic investigations are given in ref. 4.

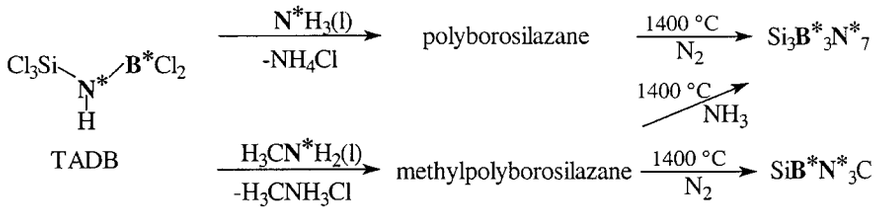

Scheme 1

In addition to the neutron experiments, X-ray diffraction experiments were applied to the same samples using high energy synchrotron radiation which in comparison to laboratory sources offers the advantage of covering a wider range of the momentum transfer Q. Thus, a better resolution in the correlation functions is achieved and, at the same time, systematic errors due to absorption effects are reduced.[8]

Experimental

X-Ray diffraction

The X-ray diffraction experiment on $Si_3B_3N_7$ was carried out at the high energy beamline BW5 of the Hamburg Synchrotron Laboratory HASYLAB. A detailed description of the experimental equipment is given in refs. 9 and 10. For monochromatization a (111)Si/$TaSi_2$ crystal was used,[11] while monitoring was performed by recording the signal from an aluminium foil placed in the incident beam with a NaI scintillation counter.

The powder sample was allowed to fill a 3 mm diameter cylindrical glass tube and placed in an aluminium vacuum-container in order to eliminate scattering due to air. The container was equipped with several capton windows, each covering a range of 20° in 2θ. Different positions were used for the different Q ranges of the diffraction pattern. For the low Q range (0.8–17.5 $Å^{-1}$) two overlapping 2θ ranges (1–10° and 9–25°) were selected. The incident energy for this Q range was 79.8(3) keV. For the high Q range (9.5–26.8 $Å^{-1}$) the chosen photon energy was 119.5(7) keV. Several scans were run to minimise errors arising from beam fluctuations.

In order to make sure that the samples constituted of isotopes in their natural abundance ($Si_3B_3N_7$) and isotopically enriched samples ($Si_3{}^{11}B_3{}^{nat}N_7$ and $Si_3{}^{11}B_3{}^{15}N_7$) are structurally identical, X-ray diffraction measurements were also performed on the latter. For the enriched sample the experimental set up was slightly different from that used for the natural sample. The NaI monitor was replaced by a diode leading to better monitoring, and the vacuum container was equipped with an aluminium window. As a consequence the whole data collection could be performed in one 2θ scan. A (111)Si(Ge) gradient crystal was used as a monochromator.[12]

Neutron diffraction

The neutron diffraction experiments were carried out at the SANDALS diffractometer at ISIS.[13] The instrument was equipped with 1060 detectors grouped into 14 detector banks at different scattering angles. A more detailed description of the instrument is given in ref. 13. The powder samples were allowed to fill a cylindrical vanadium tube of 11 mm diameter and placed in a vacuum container.

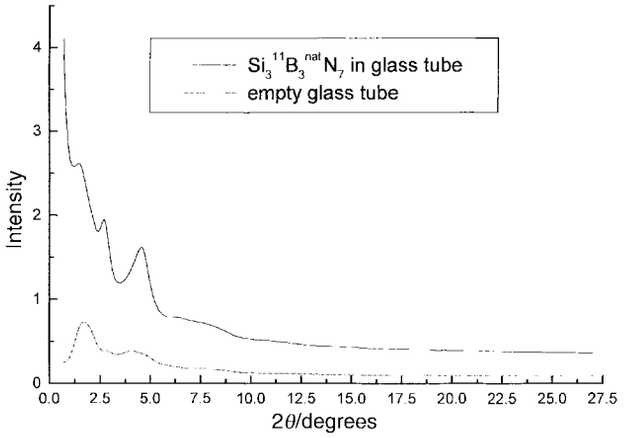

Fig. 1 High energy [$E = 119.5(7)$ keV] raw X-ray data for $Si_3{}^{11}B_3{}^{nat}N_7$ in a glass tube (upper curve) and of the empty glass tube (lower curve).

Data treatment and results

X-Ray diffraction

Raw data treatment. Owing to problems with the stability of the monitor each scan for natural $Si_3B_3N_7$ was normalised to the beam current of the DORIS synchrotron. For the isotopic samples $Si_3{}^{11}B_3{}^{15}N_7$ and $Si_3{}^{11}B_3{}^{nat}N_7$ the more stable signal of the diode was used for monitoring. As an example, Fig. 1 shows the raw X-ray data for $Si_3{}^{11}B_3{}^{nat}N_7$, and the background resulting from the scattering of the empty glass tube, after summation of the individual scans and correction for the tangential movement of the detector. The data were corrected for absorption, multiple scattering, polarisation of the incident beam, inelastic scattering and for the background as described in ref. 8.

Structure factors. The momentum transfer Q ($Å^{-1}$) for scattering X-rays with energy E (keV) to the angle 2θ is (h = Planck's constant; c = speed of light):

$$Q = (4\pi/hc)E \sin\theta = 1.0135E \sin\theta$$

The total FZ structure factor $S(Q)$ according to Faber–Ziman[14] follows from the coherently scattered intensity per atom $I_{co}(Q)$:

$$S(Q) = \frac{I_{co}(Q) - [\langle f(Q)^2\rangle - \langle f(Q)\rangle^2]}{\langle f(Q)\rangle^2}$$

with

$$\langle f(Q)^2\rangle = \sum_{i=1}^{n} c_i f_i^2, \quad \langle f(Q)\rangle = \sum_{i=1}^{n} c_i f_i$$

where $f_i(Q)$ is the atomic scattering amplitude[15] of component i, c_i the atomic fraction of component i and n the number of different atomic scatterers.

The total FZ structure factor can be expressed as a weighted sum of the partial structure factors $S_{ij}(Q)$, *e.g.* for an n-atomic system:

$$S(Q) = \frac{1}{\langle f(Q)\rangle^2} \cdot \sum_{i=1}^{n}\sum_{j=1}^{n} c_i c_j f_i(Q) f_j(Q) S_{ij}(Q)$$

$$= \sum_{i=1}^{n}\sum_{j=1}^{n} W_{ij}(Q) S_{ij}(Q)$$

For X-ray scattering the weighting factors W_{ij} are Q-dependent, and as a reasonable Q-independent approximation the average over the Q-range considered has been applied. Raw data treatment and normalisation yield the total structure factor $S(Q)$.

Pair correlation functions. From $S(Q)$ one obtains the total pair correlation function

$$G(R) = \frac{2}{\pi}\int_0^{\infty} Q[S(Q) - 1]\ \sin(QR)\ \mathrm{d}Q$$

where R is the distance in real space. $G(R)$ finally yields the radial distribution function RDF(R) which is a weighted sum of the partial functions $\mathrm{RDF}_{ij}(R)$

$$\mathrm{RDF}(R) = 4\pi\rho_0 R^2 + R{\cdot}G(R) = \sum_{i=1}^{n}\sum_{j=1}^{n} W_{ij}(R) \times \mathrm{RDF}_{ij}(R)$$

with ρ_0 equal to the mean number density. By applying the above approximation for the Q-dependent weighting factors the $W_{ij}(R)$ terms also become R-independent. From the peak area obtained by by integrating over the peaks in $\mathrm{RDF}_{ij}(R)$ one can obtain partial coordination numbers, the number of atoms j in a spherical shell of thickness $\Delta R = R_2 - R_1$ at the distance R

from a central atom i:

$$Z_{ij}(R_1, R_2) = \int_{R_1}^{R_2} \mathrm{RDF}_{ij}(R)\,\mathrm{d}R$$

Coordination numbers are usually obtained by fitting Gaussian functions to the peaks in the partial RDF_{ij}. In a good approximation the area A_{ij} under a peak is correlated to the partial coordination number Z_{ij} by

$$A_{ij} = \frac{Z_{ij} W_{ij}}{c_j}$$

If the maxima in the total RDF are well separated and related to a definite atomic distance one can also extract partial coordination numbers out of this total RDF function. As a reasonable approximation, the areas A_{ij} have been normalised to mean weighting factors W_{ij} averaged over the Q-range of the Fourier transform. The weighting factors of the different samples for the two different types of radiation are compiled in Table 1.

Fig. 2 shows the X-ray pair correlation functions $G(R)$ of amorphous $Si_3B_3N_7$, $Si_3{}^{11}B_3{}^{nat}N_7$ and $Si_3{}^{11}B_3{}^{15}N_7$ as obtained from the Faber–Ziman structure factors by integration up to $Q_{max} = 24.54$, 22.44 and 21.54 $Å^{-1}$, respectively.

Table 2 lists structural data as derived from the pair correlation functions along with data from electron diffraction experiments. The results are discussed below.

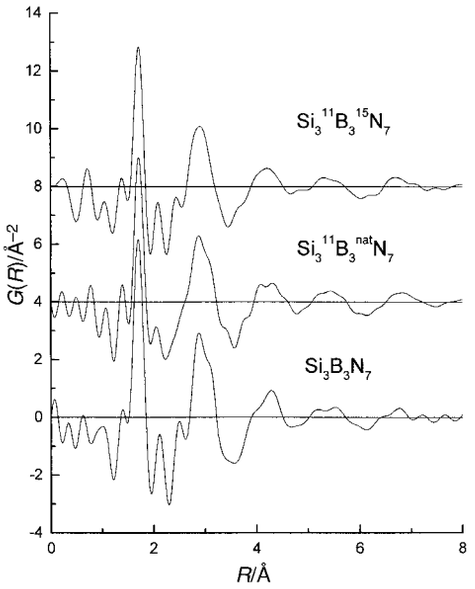

Fig. 2 Total pair correlation functions $G(R)$ for amorphous $Si_3B_3N_7$ (lower curve), $Si_3{}^{11}B_3{}^{nat}N_7$ (middle curve) and $Si_3{}^{11}B_3{}^{15}N_7$ (upper curve).

Neutron diffraction

Raw data treatment. The raw data were analysed using the ATLAS[13] program package. Only intensities recorded with a stability of better than 1% (846 out of 1070) were included in the data analysis. In calculating the total differential cross-section of the samples, corrections for attenuation and multiple scattering in the samples and cell were applied. The background and the container scattering were subtracted. The sample scattering was normalised to a vanadium standard using an effective density for the powder that corresponded to the known total scattering cross-section of the sample at high Q values. After subtracting the single-atom scattering, the resulting interference functions of each detector group overlapped and were merged (neglecting two groups at low scattering angles with poor statistics, leaving 12 groups with 806 detectors).

Differential cross-sections and total correlation functions. The quantity measured in an neutron scattering experiment is the differential cross-section $\mathrm{d}\sigma/\mathrm{d}\Omega$ and is correlated to

Table 1 Weighting factors W_{ij} from X-ray (X) and neutron (n) radiation for amorphous $Si_3B_3N_7$, $Si_3{}^{11}B_3{}^{nat}N_7$ and $Si_3{}^{11}B_3{}^{15}N_7$

	N–N	Si–N	B–N	Si–Si	Si–B	B–B
$Si_3B_3N_7$ (X); $Q=0$	0.213	0.366	0.131	0.157	0.112	0.02
$Si_3B_3N_7$ (X); Q_{mean}	0.202	0.376	0.117	0.179	0.109	0.017
$Si_3{}^{11}B_3{}^{nat}N_7$ (n)	0.449	0.171	0.271	0.016	0.052	0.041
$Si_3{}^{11}B_3{}^{15}N_7$ (n)	0.341	0.188	0.298	0.026	0.082	0.065

Table 2 Total pair correlation functions $G(R)$, positions R_i/Å, FWHM ΔR_i/Å, areas A_{ij} and partial coordination numbers Z_{ij} for amorphous $Si_3B_3N_7$, $Si_3{}^{11}B_3{}^{nat}N_7$ and $Si_3{}^{11}B_3{}^{15}N_7$

	X-ray-diffraction			Electron diffraction[16]	
	$Si_3B_3N_7$	$Si_3{}^{11}B_3{}^{nat}N_7$	$Si_3{}^{11}B_3{}^{15}N_7$	$Si_3B_3N_7$	Assignment[a]
R_1	1.411(3)	1.400(1)	1.406(4)	1.44	B–N
ΔR_1	0.164(7)	0.136(1)	0.176(1)		
A_1	0.73(2)	0.621(6)	0.61(3)		
Z_{NB}	1.4	1.2	1.2		
Z_{BN}	3.4	2.9	2.8		
R_2	1.707(1)	1.719(1)	1.717(1)	1.72	Si–N
ΔR_2	0.190(2)	0.179(1)	0.173(2)		
A_2	3.61(3)	2.67(1)	2.60(3)		
Z_{NSi}	2.2	1.6	1.6		
Z_{SiN}	5.2	3.8	3.7		
R_3	2.503(4)	2.55(1) shoulder	2.437(3)	—	N–N (hex. BN) (B–B)
ΔR_3	0.126(8)	0.242(9)	0.118(6)		
R_4	2.887(9)	2.885(4)	2.88(4)	2.91	N–N (Si_3N_4) (Si–Si)
ΔR_4	0.28(1)	0.30(1)	0.40(3)		
R_5	4.271(3)	4.246(8)	4.348(3)	4.3	
ΔR_5	0.314(4)	0.31(6)	1.095(7)		

[a]Assignments in parentheses are tentative.

the FZ structure factor by

$$S(Q) = \frac{d\sigma/d\Omega}{\langle b^2 \rangle}$$

where b is the average coherent scattering length of the atomic components in the sample.

Fig. 3 shows the differential cross-sections $d\sigma/d\Omega$ of amorphous $Si_3{}^{11}B_3{}^{nat}N_7$ and $Si_3{}^{11}B_3{}^{15}N_7$ obtained by neutron diffraction while Fig. 4 shows the total pair correlation functions $G(R)$ of $Si_3{}^{11}B_3{}^{nat}N_7$ and $Si_3{}^{11}B_3{}^{15}N_7$, which are the Fourier transforms of the respective total FZ structure factors $S(Q)$. Numerical data are compiled in Table 3.

First order difference function. Applying the difference technique, as pioneered by Soper *et al.*,[17] detailed information can be obtained even for multinary systems. By taking the difference of the intensities, measured on two samples of different isotopic concentrations, only terms including the correlation of the substituted atom species are present in the difference function. Thus for $Si_3B_3N_7$ the difference contains only the nitrogen-centred correlations and we can write[18] (X = Si,B):

$$\Delta I(Q) = \text{const.} + \alpha[S_{NN}(Q) - 1] + \beta[S_{NX}(Q) - 1] + \ldots$$

where $\alpha = c_N{}^2[b(^{nat}N)^2 - b(^{15}N)^2]$, $\beta = 2\,c_N c_X[b(^{nat}N) - b(^{15}N)]\,b_X$.

By Fourier transforming ΔI one obtains a function $\Delta G_N(R)$, that is a weighted sum of N-centred partials. Fig. 5 shows the first order difference function $\Delta_N(Q)$ and Fig. 6 its Fourier transform $\Delta G_N(R)$. Table 4 is a compilation of peak data from $\Delta G_N(R)$.

Discussion

In order to facilitate the explanation of the results, Table 5 lists the possible chain configurations for the ceramic $Si_3B_3N_7$.

By comparing the pair distribution functions obtained from the X-ray diffraction patterns of the three isotopically differently synthesised samples, $Si_3B_3N_7$, $Si_3{}^{11}B_3{}^{nat}N_7$ and $Si_3{}^{11}B_3{}^{15}N_7$, it is evident that the results are virtually identical. For the short range order they are in excellent agreement with the results as obtained from other techniques such as *e.g.* MAS NMR.

The main maximum at *ca.* 1.71 Å for $Si_3B_3N_7$ and *ca.* 1.72 Å for the two isotopically enriched samples represents the nearest neighbour distance of Si and N in an SiN_4 tetrahedron, as has been found for crystalline Si_3N_4 (1.70–1.78 Å[19]). The weaker maximum at *ca.* 1.40 Å for $Si_3{}^{11}B_3{}^{nat}N_7$ and *ca.* 1.41 Å for $Si_3B_3N_7$ and $Si_3{}^{11}B_3{}^{15}N_7$ can be related to the B–N distance in a BN_3 triangle as has been reported for hexagonal BN (1.446 Å[20]).

The partial coordination numbers obtained from the Gaussian fits to these two maxima in the RDF of $Si_3{}^{11}B_3{}^{nat}N_7$ and $Si_3{}^{11}B_3{}^{15}N_7$ ($Z_{BN} = 2.9/2.8$, $Z_{SiN} = 3.8/3.7$, $Z_{NB} = 1.2$, $Z_{NSi} = 1.6$) are in accord within the limits of the experimental error, and essentially match the expected coordination numbers. The determination of partial coordination numbers from the RDF of the non-isotopic sample give values $Z_{BN} = 3.4$, $Z_{SiN} = 5.2$, $Z_{NB} = 1.4$ and $Z_{NSi} = 2.2$. These are slightly higher than expected, possibly because of the difference in the experimental set up as described above.

The second coordination sphere is dominated by a peak at *ca.* 2.88 Å, which can be related to the N–N distance within a SiN_4 tetrahedron (crystalline Si_3N_4: 2.78–2.98 Å[19]). This peak

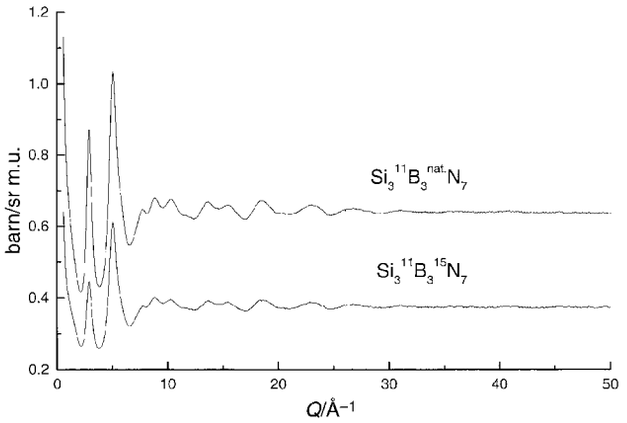

Fig. 3 Differential cross-sections from neutron diffraction for amorphous $Si_3{}^{11}B_3{}^{nat}N_7$ (upper curve) and $Si_3{}^{11}B_3{}^{15}N_7$ (lower curve) (m.u. = molecular units).

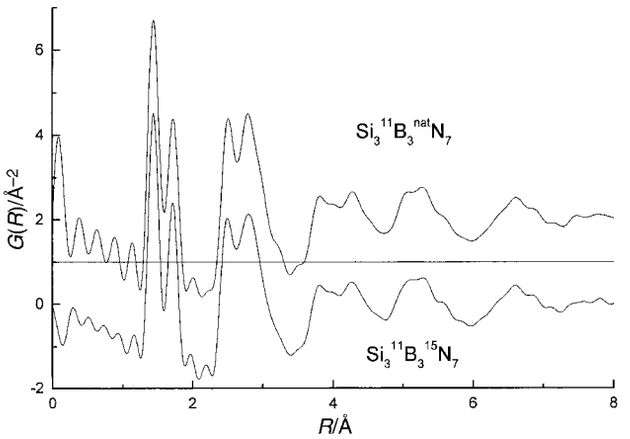

Fig. 4 Total pair correlation functions from neutron diffraction for amorphous $Si_3{}^{11}B_3{}^{nat}N_7$ (upper curve) and $Si_3{}^{11}B_3{}^{15}N_7$ (lower curve).

Table 3 Total pair correlation functions $G(R)$, neutron diffraction positions R_i/Å, FWHM ΔR_i/Å, areas A_{ij} and partial coordination numbers Z_{ij} for amorphous $Si_3{}^{11}B_3{}^{nat}N_7$ and $Si_3{}^{11}B_3{}^{15}N_7$

	$Si_3{}^{11}B_3{}^{nat}N_7$	$Si_3{}^{11}B_3{}^{15}N_7$		$Si_3{}^{11}B_3{}^{nat}N$[a]	$Si_3{}^{11}B_3{}^{15}N_7$	Assignment[b]
R_1	1.447(1)	1.446(1)	ΔR_1	0.134(2)	0.140(2)	B–N
A_1	1.41(2)	1.53(2)				
Z_{NB}	1.2	1.2	Z_{BN}	2.8	2.8	
R_2	1.718(1)	1.721(1)	ΔR_2	0.131(3)	0.141(3)	Si–N
A_2	1.09(2)	1.17(2)				
Z_{Nsi}	1.5	1.4	Z_{SiN}	3.4	3.4	
R_3	2.477(1)	2.487(2)	ΔR_3	0.156(6)	0.160(4)	N–N/B–B
A_3	1.5(2)	1.73(3)	Z_{NN}/Z_{BB}	1.65	2.3	
R_4	2.77(5)	2.784(4)	ΔR_4	0.33(6)	0.30(1)	N–N (Si–B)
A_4	3.8(1)	3.4(3)	Z_{NN}	4.6	5.4	
R_5	3.81(1)	3.792(7)	ΔR_5	0.32(5)	0.29(1)	
R_6	4.25(9)	4.25(3)	ΔR_6	0.5(2)	0.6(1)	
R_7	5.24(1)	5.22(1)	ΔR_7	0.55(7)	0.56(6)	

[a]Ref. 7. [b]Assignments in parentheses are tentative.

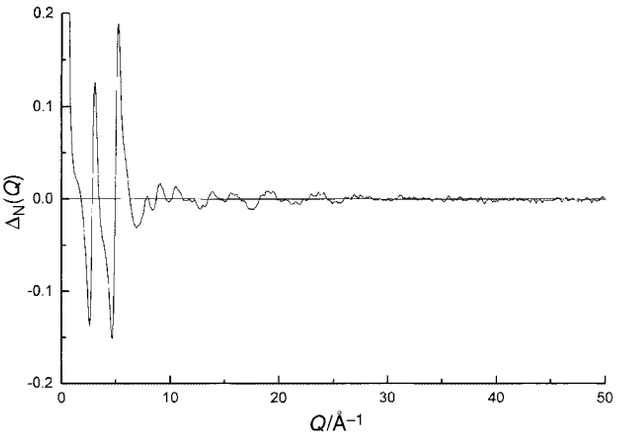

Fig. 5 First order neutron difference function $\Delta_N(Q)$ for $Si_3{}^{11}B_3N_7$.

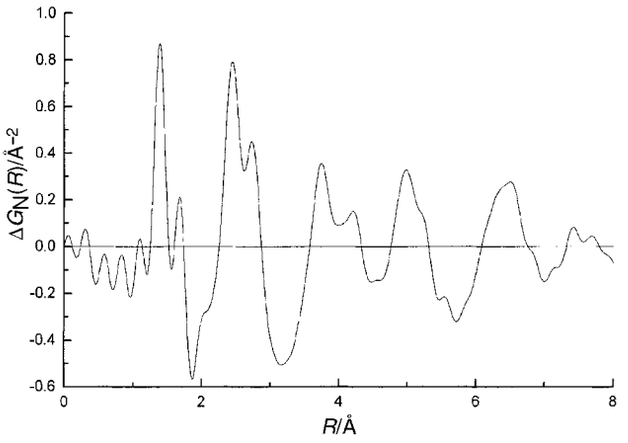

Fig. 6 Fourier transform $\Delta G_M(R)$ of the first order neutron difference ($Si_3{}^{11}B_3{}^{nat}N_7-Si_3{}^{11}B_3{}^{15}N_7$).

includes as a shoulder a contribution of an Si–Si distance of two corner sharing tetrahedra. Other distances listed in Table 2 can only be interpreted by comparing with the neutron results discussed below.

The first coordination distances in the total pair correlation functions as obtained from the neutron diffraction on $Si_3{}^{11}B_3{}^{nat}N_7$ and $Si_3{}^{11}B_3{}^{15}N_7$ are *ca.* 1.45 Å for the B–N distance and *ca.* 1.72 Å for the Si–N distance. Also, the partial coordination numbers ($Z_{BN}=2.8$, $Z_{SiN}=3.4$, $Z_{NB}=1.2$ and $Z_{NSi}=1.5/1.4$) are comparable with the X-ray results.

The second coordination sphere shows a clear splitting into two well separated maxima, one at *ca.* 2.48/2.49 Å, the other at 2.77/2.78 Å with the latter being broadened with the appearance of a shoulder to longer distances. The first can be related to an N–N distance with both N-atoms coordinated to a boron atom or a B–B distance with both atoms coordinated to a nitrogen atom while the second can be related to an N–N distance with both N-atoms coordinated to a silicon. The Gaussian fits to these maxima in the RDF yield the partial coordination numbers $Z_{NN}(B)=1.7/2.3$ for the first maximum, and $Z_{NN}(Si)=4.6/5.4$ for the second. The reason for the large difference from the expected value (*ca.* 3) for $Z_{NN}(Si)$ lies in the contribution of a shoulder to the corresponding peak area. This fact will be discussed in context with the difference function below. In the region of the third coordination shell there is a maximum at *ca.* 3.81/3.80 Å and one at 4.25 Å.

Table 4 Fourier transform of the first order difference $\Delta G_N(R)$; positions R_i/Å and FWHM ΔR_i/Å for amorphous $Si_3{}^{11}B_3N_7$

				Assignment
R_1	1.398(7)	ΔR_1	0.155(1)	B–N
R_2	1.683(1)	ΔR_2	0.142(2)	Si–N
R_3	2.44(1)	ΔR_3	0.18(1)	N–N
R_4	2.731(5)	ΔR_4	0.32(1)	N–N
R_5	3.76(1)	ΔR_5	0.46(1)	Si/B–N
R_6	4.290(7)	ΔR_6	0.41(2)	B/Si–N
R_7	5.085(7)	ΔR_7	0.93(2)	N–N
R_8	6.595(2)	ΔR_8	1.31(1)	

The peaks in the Fourier transform of the first order difference function are in accord with the values given above as derived for the first and second coordination from the total correlation functions: $R_{BN}=1.40$ Å, $R_{SiN}=1.68$ Å, $R_{NN}(B)=2.44$ Å and $R_{NN}(Si)=2.73$ Å. Upon comparing the second coordination maxima in Fig. 6 (first order difference) with the second coordination peak in Fig. 4 (total functions) significant differences become apparent. In the total function, the two maxima are approximately equal in height, whereas in the difference function the second is lower and narrower compared to the total functions. This leads to the conclusion that in the total functions there is a contribution of a distance between non-nitrogen atoms (most probably Si–B) to this maximum.

Furthermore, as a result of application of the first order difference technique, some information on the medium range order can be extracted. Looking at the third coordination shell the difference function shows a clear splitting into two maxima at 3.76 Å and 4.29 Å. These two distances can be assigned to atomic pairs by comparing with distances in the binary crystalline phases[19,20] and with the geometry of the precursor molecule TADB as obtained from quantum mechanic calculations.[21] In the difference function, only nitrogen-coordinations appear, so these maxima can be assigned to Si–N and B–N pairs connected *via* three bonds. Configurations with at least two of the three bonds being B–N contribute to the first peak whereas if at least two of them are Si–N bonds a contribution to the second peak results. A complete fitting of the whole peak region at *ca.* 4 Å requires four Gaussian functions, each representing a possible Si/B–N pair (Table 6). The dihedral angle distributions for all these four configurations range from 97 to 180° within the 2σ criterion. As an example, Fig. 7 shows the correlation of the dihedral angle and the Si–N separation for the N–B–N–Si chain.

The broad but nevertheless strong maximum at 5.085 Å, representing the fourth coordination shell, is a superposition of the three distance distributions for chains connected *via* four bonds (N–B–N–B–N, N–Si–N–B–N and N–Si–N–Si–N). Since

Table 5 Possible chain configurations in $Si_3B_3N_7$. Chains giving a contribution to the neutron first order difference ($^{14}N-{}^{15}N$) are italicized

1st coordination	2nd coordination	3rd coordination	4th coordination
B–N	B–N–B	*B–N–B–N*	*N–B–N–B–N*
Si–N	*N–B–N*	*Si–N–B–N*	B–N–B–N–B
	B–N–Si	*B–N–Si–N*	*N–B–N–Si–N*
	N–Si–N	*Si–N–Si–N*	B–N–Si–N–B
	Si–N–Si		B–N–Si–N–Si
			N–Si–N–Si–N
			Si–N–Si–N–Si
			Si–N–B–N–Si

Table 6 Fourier transform of the first order difference $\Delta G_N(R)$, Gaussian fits to the third coordination shell, positions R_i/Å, FWHM ΔR_i/Å and 2σ ranges of the dihedral angle Φ/° distributions for amorphous $Si_3B_3N_7$

				Assignment	Φ	2σ range
R_{5a}	3.49	ΔR_{5a}	0.16	N–B–N–B	119	107–132
R_{5b}	3.73	ΔR_{5b}	0.25	N–B–N–Si	113	97–132
R_{6a}	4.05	ΔR_{6a}	0.26	N–Si–N–B	150	127–180
R_{6b}	4.25	ΔR_{6b}	0.17	N–Si–N–Si	136	124–152

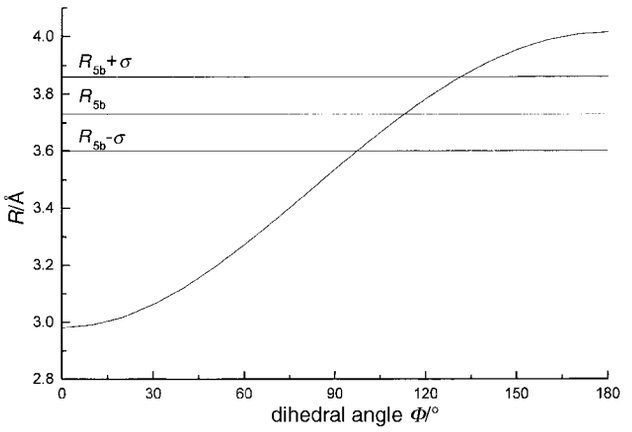

Fig. 7 Dihedral angle Φ distribution of the N–B–N–Si chain in $Si_3B_3N_7$ obtained from the first order neutron difference.

in the first order difference, only coordinations including nitrogen emerge, only N–N pairs can contribute to this shell.

Conclusion

High energy X-ray diffraction on samples of $Si_3B_3N_7$ synthesised independently do not show significant structural differences. The peaks in the first coordination shell at *ca.* 1.41 and 1.71 Å and the partial coordination numbers determined from the peak areas are in agreement with NMR results and indicate boron being in a trigonally planar environment of nitrogen and silicon being tetrahedrally coordinated. In the second coordination shell the maximum at *ca.* 2.89 Å represents the N–N distance for two adjacent nitrogen atoms coordinated to silicon. The significance of the weak maximum at *ca.* 2.5 Å has been confirmed by the results from neutron diffraction, where the total distribution functions show two separated maxima at *ca.* 2.48 and 2.78 Å. The first can clearly be assigned to a N–N distance in a BN_3 triangle and the partial coordination numbers of $Z_{NN} = 1.65/2.3$ are in agreement with expected values, within experimental error. While the second maximum could be interpreted as described above (N–N distance in a SiN_4 tetrahedron) since the partial coordination numbers were too high ($Z_{NN} = 4.6/5.4$) this peak seems to include a further atomic distance (Si–B). This was confirmed by the first order difference results.

From the neutron difference function, additional information concerning the higher coordination shells could be extracted. Maxima at 3.76 and 4.29 Å result from Si–N or B–N pairs connected *via* three bonds. If at least two of these are B–N bonds it gives a contribution to the first peak, whereas if there are at least two Si–N bonds a contribution to the second peak is observed. A complete fitting of this peak region yielded four pair distances representing all possible chain configurations in the third coordination shell. The dihedral angle distributions gave no hint at a preferred chain configuration.

Acccording to these results the following structural model for $Si_3B_3N_7$ may be described: almost trigonal planar BN_3 units and slightly distorted SiN_4 tetrahedra bridged *via* common nitrogen atoms form a three-dimensional random network in which silicon and boron atoms are homogeneously distributed.[16]

Acknowledgements

We are grateful to R. Weisbarth and M. Theis for assisting with the X-ray experiment. Financial support from the BMBF under project no. JA34.07K and from DESY is also gratefully acknowledged.

References

1 M. Jansen, *Solid State Ionics*, 1997, **101–103**, 1.
2 H. P. Baldus and M. Jansen, *Angew. Chem.*, 1997, **109**, 338; *Angew. Chem., Int. Ed. Engl.*, 1997, **36**, 255.
3 H. P. Baldus, O. Wagner and M. Jansen, *Mater. Res. Soc. Symp. Proc.*, 1992, **271**, 821.
4 U. Müller, W. Hoffbauer and M. Jansen, *Chem. Mater.*, submitted.
5 P. Lamparter and S. Steeb, in *Material Science and Technology*, VCH, Weinheim, 1993, vol. 1, p. 217.
6 C. J. Benmore and P. S. Salmon, *Phys. Rev. Lett.*, 1994, **73**, 264.
7 V. F. Sears, *Thermal-Neutron Scattering Lengths and Cross Sections for Condensed-Matter Research*, Atomic Energy of Canada Limited, Chalk River, Ontario, Canada, 1984, AECL Report No. 8490.
8 H. F. Poulsen, J. Neuefeind, H.-B. Neumann, J. R. Schneider and M. D. Zeidler, *J. Non-Cryst. Solids*, 1995, **188**, 63.
9 J. Neuefeind, K. Tödheide, A. Lemke and H. Bertagnolli, *J. Non-Cryst. Solids*, 1998, **224**, 205.
10 R. Bouchard, D. Hupfeld, T. Lippmann, J. Neuefeind, H.-B. Neumann, H. F. Poulsen, U. Rütt, T. Schmidt, J. R. Schneider, J. Süßenbach and M. v. Zimmermann, *J. Synchrotron Radiat.*, 1998, **5**, 90.
11 H.-B. Neumann, J. R. Schneider, J. Süssenbach, S. R. Stock and Z. U. Rek, *Nucl. Instrum. Methods A*, 1996, **372**, 551.
12 S. Keitel, C. C. Retsch, T. Niemöller, J. R. Schneider, N. V. Abrasimov, S. N. Rossolenko and H. Riemann, *Nucl. Instrum. Methods A*, 1998, **414**, 427.
13 A. K. Soper, W. S. Howells and A. C. Hannon, *Analysis of Time-of-flight Diffraction Data from Liquid and Amorphous Samples ATLAS 1.0*, ISIS Facility, RAL, Chilton, Didcot, 1997.
14 T. E. Faber and J. M. Ziman, *Philos. Mag.*, 1965, **11**, 153.
15 *International Tables for Crystallography*, ed. A. J. C. Wilson, Kluwer Academic, Dordrecht, 1992.
16 D. Heinemann, W. Assenmacher, W. Mader, M. Kroschel and M. Jansen, *J. Mater. Res.*, submitted.
17 A. K. Soper, G. W. Neilson, J. E. Enderby and R. A. Howe, *J. Phys. C*, 1977, **10**, 1793.
18 P. H. Gaskell, in *Proc. ILL/ESRF Workshop on Methods in the Determination of Partial Structure Factors, Grenoble 1992*, ed. J. B. Suck, P. Chieux, D. Raoux and C. Riekel, World Scientific, Singapore, 1993, p. 34.
19 I. Kohatsu and J. W. McCauley, *Mater. Res. Bull.*, 1974, **9**, 917.
20 R. S. Pease, *Acta Crystallogr., Sect. A*, 1952, **5**, 356.
21 M. Mühlhaeuser, M. Gastreich, C. M. Marian, H. Jüngermann and M. Jansen, *J. Phys. Chem.*, 1996, **100**, 16 551.

Paper 9/02346A